

## THE EFFECT OF MECHANOCHEMICAL ACTIVATION ON THE REACTIVITY IN THE MgO–Al<sub>2</sub>O<sub>3</sub>–SiO<sub>2</sub> SYSTEM

C. A. d'Azevedo<sup>1,2</sup>, F. M. S. Garrido<sup>2</sup> and M. E. Medeiros<sup>2\*</sup>

<sup>1</sup>Instituto de Pesquisas da Marinha – Rua Ipirú no. 2, Ilha do Governador, 21931-090 Rio de Janeiro, Brazil

<sup>2</sup>Departamento de Química Inorgânica, Instituto de Química, Universidade Federal do Rio de Janeiro, Ilha do Fundão 21945-970 Rio de Janeiro, Brazil

Samples of the MgO–Al<sub>2</sub>O<sub>3</sub>–SiO<sub>2</sub> ternary system, constituted by 28.5 mol% of MgO, 28.5 mol% of Al<sub>2</sub>O<sub>3</sub> and 43 mol% of SiO<sub>2</sub>, were activated in a roll mill and calcined at different temperatures. The influence of the grinding time, the used SiO<sub>2</sub> precursor and activation medium, furthermore the mass ratio between the powdered sample and zirconia cylinders was investigated on the reactivity of the MgO–Al<sub>2</sub>O<sub>3</sub>–SiO<sub>2</sub> ternary system. FTIR spectra and the X-ray powder diffraction patterns indicates the formation of Mg(OH)<sub>2</sub> at 393 K, of forsterite (MgSi<sub>2</sub>O<sub>5</sub>) and enstatite (MgSiO<sub>3</sub>) at 1223 K and of spinel (MgAl<sub>2</sub>O<sub>4</sub>) between 1223 and 1523 K in some samples. The presence of cordierite (Mg<sub>2</sub>Al<sub>2</sub>Si<sub>5</sub>O<sub>18</sub>) was observed at 1523 K, a reaction pathway concerning its formation was proposed.

**Keywords:** cordierite, enstatite, mechanochemistry, spinel

### Introduction

The energy transfer during the grinding process and its effect on the reactivity was the subject of several studies, usually using high-energy mills with speeds higher than 500 rpm. Besides, the increase in the homogeneity and the variation of the particle size, the intensity of the locally applied force over a determined powder volume at the contact point during the impact, determines mechanochemical activation of the powder. The formation of defects in the crystalline network and of amorphous phases is common in this process. In some special cases, reactions between the mixture components can occur during the grinding process [1–7].

Cordierite based ceramics in the MgO–Al<sub>2</sub>O<sub>3</sub>–SiO<sub>2</sub> ternary system have great economic importance. Cordierite composition can vary between the two formulas 2MgO·2Al<sub>2</sub>O<sub>3</sub>·5SiO<sub>2</sub> and MgO·Al<sub>2</sub>O<sub>3</sub>·3SiO<sub>2</sub>. In these ceramics frequently secondary crystalline phases, such as corundum, mullite, spinel, forsterite, enstatite and cristobalite are present [7–12]. As a consequence, the properties of these ceramics strongly depend on the composition, the presence of additives and manufacturing techniques. Recently, the importance of spinel in the cordierite formation process was discussed [7, 9–11]. Some authors proposed that cordierite is formed from the reaction between spinel and a silica precursor phase [7, 9]. However, other authors suggest that the application of additives allows the direct synthesis of cordierite, either by the reaction between MgO, Al<sub>2</sub>O<sub>3</sub> and SiO<sub>2</sub> [10] or by the reaction between enstatite and alumina [11].

In this work, the mechanochemical activation of the MgO–Al<sub>2</sub>O<sub>3</sub>–SiO<sub>2</sub> ternary system was studied. The objective was to produce ceramics based on the cordierite where spinel as the main secondary phase is present, and to elucidate the influence of the spinel phase on the cordierite formation.

### Experimental

#### Materials and methods

Silicic acid (H<sub>4</sub>SiO<sub>4</sub>) (Merck, dehydrated by treatment with Merck concentrated perchloric acid [12]) and calcined at 1173 K for 4 h was used as silica (SiO<sub>2</sub>) precursor in the case of  $\alpha$  type samples. Another silica precursor was the Merck silica gel HF<sub>254</sub> (Type 60) and used as it was received, for  $\beta$  type samples. The magnesium oxide precursor (MgO, P.A. Merck) was submitted to a thermal treatment at 823 K for 4 h, transforming to periclase [13]. The aluminum oxide precursor (Al<sub>2</sub>O<sub>3</sub>, Ridel-of-Haën) was calcined at 1473 K (4 h) and was used in the  $\alpha$ -corundum formation ( $\alpha$ -Al<sub>2</sub>O<sub>3</sub>) [12, 14].

On the grinding process, 10 to 4.5 g of the oxide mixture, with equal composition 28.5 mol% of MgO, 28.5 mol% of Al<sub>2</sub>O<sub>3</sub> and 43 mol% of SiO<sub>2</sub>, were placed into a Nalgene bottle, together with the grinding elements. This composition, with an excess of MgO and Al<sub>2</sub>O<sub>3</sub>, was used to investigate the influence of the spinel phase on the cordierite formation. The grinding was performed in a US Stoneware roll mill at

\* Author for correspondence: martam@iq.ufjf.br

100 rpm. Zirconia cylinders (Netzsch) with 1 cm of diameter and 1 cm of length were used as grinding elements in the place of zirconia spheres, to increase the shock area [7]. Absolute ethyl alcohol (P.A. Grupo Química) and distilled and deionized water (MILLI-Q Water System equipment – Millipore) were used as 'activation medium'. Table 1 presents the applied experimental conditions for grinding for each sample.

The samples were heated for 2 h at 393, 1223, 1423, 1523 and 1623 K. The heating process was performed in two stages: 1) Starting from ambient temperature using 6 K min<sup>-1</sup> of heating rate ( $\beta$ ) to reach 423 K, and keeping the samples at 423 K for 1 h; 2) Starting from 423 K with  $\beta=10$  K min<sup>-1</sup> until to reach the temperature of calcination and remaining there for 2 h. A Thermolyne F46240CM electric oven was used for all the thermal treatments.

The infrared spectra were obtained with a 4 cm<sup>-1</sup> resolution using a FTIR Nicolet Magna 760 Spectrophotometer, and the KBr disc technique. The crystalline phases were subjected to X-ray diffraction (XRD) analysis using a Rigaku Miniflex Diffractometer with Ni-filtered CuK $\alpha$  radiation, with a scanning speed of 2° min<sup>-1</sup>.

## Results and discussion

### Dehydrated and calcined silicic acid as SiO<sub>2</sub> precursor

Table 2 shows the XRD and FTIR results of  $\alpha$ D0– $\alpha$ D5 serial heated to different temperatures. The XRD re-

sults for the samples heated to 394 K and for the samples calcinated at 1223 K (Table 2 and Fig. 1) show a progressive decrease in the relative intensity of  $2\theta=42.90^\circ$  peak. This can be accompanied with a progressive amorphization of the periclase (MgO) [13], which takes place as a consequence of the increase on the grinding time and of the reduction of the  $M/C$  ratio.

For the samples heat-treated at 1223 K (Table 2 and Fig. 1), the observed predominant crystalline phase was  $\alpha$ -Al<sub>2</sub>O<sub>3</sub> [14]. In addition, different amounts of periclase (MgO) were also observed. For the  $\alpha$ D0 sample the amount of periclase was larger. For all the samples the formation of a small amount of Mg and Al spinel (MgAl<sub>2</sub>O<sub>4</sub>), as indicated by XRD peaks at  $2\theta=36.80$  and  $44.80^\circ$  [15] were also observed. However, with exception of the  $\alpha$ D0 sample, bands in the IR spectra (at 952 and 894 cm<sup>-1</sup>, in the region of Si-O stretching [16, 17]) as well peaks in the XRD (at  $2\theta=22.90$ , 32.30, 35.70 and  $39.80^\circ$  [18]) have been also observed, indicating the formation of a small amount of forsterite (Mg<sub>2</sub>SiO<sub>4</sub>). In addition, for  $\alpha$ D3,  $\alpha$ D4 and  $\alpha$ D5 samples, enstatite (MgSiO<sub>3</sub>) appears as a minor crystalline phase, which fact was confirmed by the IR bands at 1013 and 860 cm<sup>-1</sup>, and by the XRD peaks at  $2\theta=28.13$  and  $31.40^\circ$  [19, 20]. Enstatite occurs in a higher amount in the  $\alpha$ D5 sample, this fact underlines the importance of the degree of mechanochemical activation on the enstatite formation.

Table 2 and Figs 2 and 3 show that spinel (MgAl<sub>2</sub>O<sub>4</sub>) [15, 21] and  $\alpha$ -cristobalite [22–24] are the predominant phases in the samples calcined at 1523 K.

**Table 1** Grinding conditions

SiO <sub>2</sub> precursor	'Activation medium'	Grinding time/h	$M/C^*$ ratio	Sample
Dehydrated silicic acid	absolute ethyl alcohol	2	1/20	$\alpha$ D0
		18	1/20, 1/40	$\alpha$ D1, $\alpha$ D2
		48	1/20, 1/40, 1/80	$\alpha$ D3, $\alpha$ D4, $\alpha$ D5
	absolute ethyl alcohol	2	1/20	$\beta$ aD0
		48	1/40, 1/80	$\beta$ aD4, $\beta$ aD5
		Silica gel	mixture of absolute ethyl alcohol and water	2
48	1/40, 1/80			$\beta$ bD4, $\beta$ bD5
water	2		1/20	$\beta$ cD0
	48		1/40, 1/80	$\beta$ cD4, $\beta$ cD5

\* $M/C$ =powder mass/zirconia cylinders mass

**Table 2** Observed phases in the samples using dehydrated silicic acid as SiO<sub>2</sub> precursor

Temperature/K	Sample	Observed phases
393	AD0 to $\alpha$ D5	$\alpha$ -Al <sub>2</sub> O <sub>3</sub> , SiO <sub>2</sub> , MgO
1223	$\alpha$ D0	$\alpha$ -Al <sub>2</sub> O <sub>3</sub> , SiO <sub>2</sub> , MgO, MgAl <sub>2</sub> O <sub>4</sub>
	AD1, $\alpha$ D2 $\alpha$ D3, $\alpha$ D4, $\alpha$ D5	$\alpha$ -Al <sub>2</sub> O <sub>3</sub> , SiO <sub>2</sub> , MgO, MgAl <sub>2</sub> O <sub>4</sub> , Mg <sub>2</sub> SiO <sub>4</sub> $\alpha$ -Al <sub>2</sub> O <sub>3</sub> , SiO <sub>2</sub> , MgO, MgAl <sub>2</sub> O <sub>4</sub> , Mg <sub>2</sub> SiO <sub>4</sub> , MgSiO <sub>3</sub>
1523	$\alpha$ D0, $\alpha$ D1, $\alpha$ D2	$\alpha$ -Al <sub>2</sub> O <sub>3</sub> , $\alpha$ -SiO <sub>2</sub> , MgAl <sub>2</sub> O <sub>4</sub>
	$\alpha$ D3, $\alpha$ D4, $\alpha$ D5	$\alpha$ -Al <sub>2</sub> O <sub>3</sub> , $\alpha$ -SiO <sub>2</sub> , MgAl <sub>2</sub> O <sub>4</sub> , Mg <sub>2</sub> Al <sub>4</sub> Si <sub>5</sub> O <sub>18</sub>
1623	AD0 to $\alpha$ D5	$\alpha$ -Al <sub>2</sub> O <sub>3</sub> , $\alpha$ -SiO <sub>2</sub> , MgAl <sub>2</sub> O <sub>4</sub> , Mg <sub>2</sub> Al <sub>4</sub> Si <sub>5</sub> O <sub>18</sub>

SiO<sub>2</sub>=amorphous silica (observed by IR),  $\alpha$ -SiO<sub>2</sub>= $\alpha$ -cristobalite

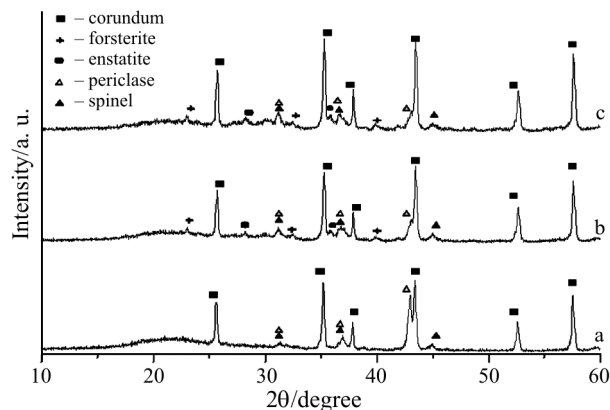


**Fig. 1** X-ray powder diffraction patterns of samples a –  $\alpha$ D0, b –  $\alpha$ D3 and c –  $\alpha$ D5 calcined at 1223 K

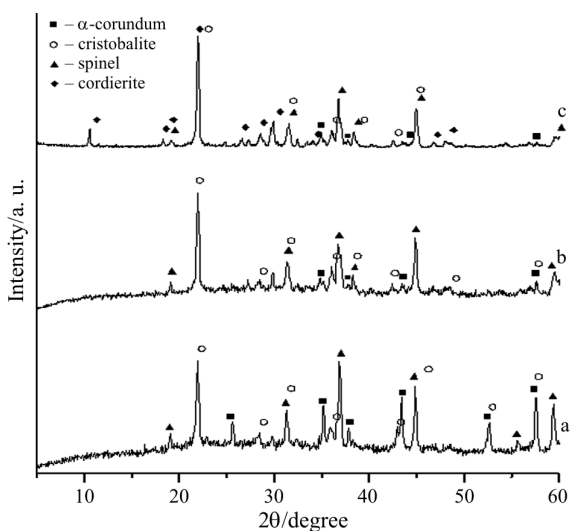


**Fig. 2** X-ray powder diffraction patterns of samples a –  $\alpha$ D0, b –  $\alpha$ D3 and c –  $\alpha$ D5 calcined at 1523 K

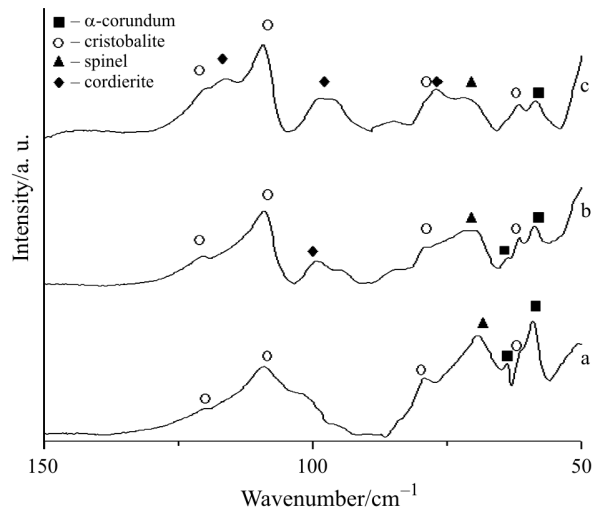


**Fig. 3** IR spectra of samples a –  $\alpha$ D0, b –  $\alpha$ D3 and c –  $\alpha$ D5 calcined at 1523 K

On the contrary in the  $\alpha$ D0 sample a great amount of  $\alpha$ -Al<sub>2</sub>O<sub>3</sub> was still observed. However, a small amount of cordierite (Mg<sub>2</sub>Al<sub>4</sub>Si<sub>5</sub>O<sub>18</sub>) was formed in  $\alpha$ D3,  $\alpha$ D4 and  $\alpha$ D5 samples, as indicated by the IR bands at 1179 cm<sup>-1</sup> (asymmetrical stretching of tetrahedral Si-O), 960 cm<sup>-1</sup> (stretching of Al-O bonding) and 770 cm<sup>-1</sup> (symmetrical stretching of Si-O bonding), and by an XRD peak at  $2\theta=28.49^\circ$  [17, 25–27]. As it can be seen in Figs 2 and 3 the amount of cordierite increases with the increase of mechanochemical activation, and therefore it is maximum in the  $\alpha$ D5 sample. This corresponds to the case where the amount of enstatite is the highest for the samples heated at 1223 K. This fact suggests a correlation between the presence of enstatite, in the samples heated at 1223 K, and the cordierite formation at 1523 K.

In all samples calcined at 1623 K the formation of cordierite (Mg<sub>2</sub>Al<sub>4</sub>Si<sub>5</sub>O<sub>18</sub>) occurred. As the grinding time increased and the *M/C* rate decreases, the amount of cordierite increased with a simultaneous diminishing of cristobalite ( $\alpha$ -SiO<sub>2</sub>). Therefore, the amount of cordierite formed in  $\alpha$ D0 sample is the lowest according to the data obtained from XRD and FTIR. These results indicate that calcined and dehydrated silicic acid is not an adequate SiO<sub>2</sub> precursor for the synthesis of cordierite at 1523 K, and hence another precursor was studied.

#### *Silica gel as SiO<sub>2</sub> precursor*

In this set of reactions another SiO<sub>2</sub> precursor and different ‘activation medium’, namely absolute ethanol (for  $\beta$ aD), 10 v/v% of deionized water in absolute ethanol (for  $\beta$ bD) and deionized water (for  $\beta$ cD). The XRD and FTIR results are summarized in Table 3 for  $\beta$ aD0– $\beta$ cD5 serial, heated at different temperatures.

For the samples were activated in the presence of water ( $\beta$ bD and  $\beta$ cD), IR band at 3700 cm<sup>-1</sup> was observed and attributed to the O–H stretching of Mg(OH)<sub>2</sub> [28]; meanwhile, an XRD peak in  $2\theta=18.59^\circ$  [29] was observed for some samples (Figs 4 and 5). These data indicated the formation of the magnesium hydroxide – Mg(OH)<sub>2</sub> – during the grinding process (Table 3). In  $\beta$ cD4 and  $\beta$ cD5 samples, as it is shown in Fig. 4, all MgO reacted since the XRD peak at  $2\theta=42.90^\circ$  was not observed [13]. For the  $\beta$ cD5 sample (Fig. 4f) the XRD peak at  $2\theta=18.59^\circ$  [29] was not observed. This fact suggests that in this sample the formed Mg(OH)<sub>2</sub> is amorphous or reacted with the SiO<sub>2</sub>, resulting an amorphous magnesium silicate as observed by MacKenzie for the MgO–SiO<sub>2</sub> system [29].

From Fig. 6 and Table 3 it can be concluded that there was no spinel formation for the samples calcined at 1223 K, as it was observed for the  $\alpha$ D samples calcined at same temperature. However, when they were

**Table 3** Observed phases in samples using silica gel as SiO<sub>2</sub> precursor

Temperature/K	Sample	Observed phases
393	βaD0, βaD4, βaD5	SiO <sub>2</sub> , α-Al <sub>2</sub> O <sub>3</sub> , MgO
	βbD0, βcD0, βbD4, βbD5	SiO <sub>2</sub> , α-Al <sub>2</sub> O <sub>3</sub> , MgO, Mg(OH) <sub>2</sub>
	βcD4	SiO <sub>2</sub> , α-Al <sub>2</sub> O <sub>3</sub> , Mg(OH) <sub>2</sub>
	βcD5	SiO <sub>2</sub> , α-Al <sub>2</sub> O <sub>3</sub> , Mg(OH) <sub>2</sub> *
1223	βaD0, βbD0	SiO <sub>2</sub> , α-Al <sub>2</sub> O <sub>3</sub> , MgO, Mg <sub>2</sub> SiO <sub>4</sub>
	βcD0	SiO <sub>2</sub> , α-Al <sub>2</sub> O <sub>3</sub> , MgO, Mg <sub>2</sub> SiO <sub>4</sub> , MgSiO <sub>3</sub>
	βaD4, βaD5	SiO <sub>2</sub> , α-Al <sub>2</sub> O <sub>3</sub> , Mg <sub>2</sub> SiO <sub>4</sub> , MgSiO <sub>3</sub>
	βbD4, βcD4, βbD5, βcD5	SiO <sub>2</sub> , α-Al <sub>2</sub> O <sub>3</sub> , MgSiO <sub>3</sub>
1423	βaD4, βbD4, βcD4, βaD5, βbD5, βcD5	α-SiO <sub>2</sub> , α-Al <sub>2</sub> O <sub>3</sub> , MgSiO <sub>3</sub> , MgAl <sub>2</sub> O <sub>4</sub>
1523	βaD0, βbD0, βcD0	α-SiO <sub>2</sub> , α-Al <sub>2</sub> O <sub>3</sub> , MgAl <sub>2</sub> O <sub>4</sub> , Mg <sub>2</sub> Al <sub>4</sub> Si <sub>5</sub> O <sub>18</sub>
	βaD4, βbD4, βcD4, βaD5	α-SiO <sub>2</sub> , α-Al <sub>2</sub> O <sub>3</sub> , MgSiO <sub>3</sub> , MgAl <sub>2</sub> O <sub>4</sub> , Mg <sub>2</sub> Al <sub>4</sub> Si <sub>5</sub> O <sub>18</sub>
	βbD5	α-SiO <sub>2</sub> , MgAl <sub>2</sub> O <sub>4</sub> , Mg <sub>2</sub> Al <sub>4</sub> Si <sub>5</sub> O <sub>18</sub>
	βcD5	MgAl <sub>2</sub> O <sub>4</sub> , Mg <sub>2</sub> Al <sub>4</sub> Si <sub>5</sub> O <sub>18</sub>

SiO<sub>2</sub>=amorphous silica, \*amorphous Mg(OH)<sub>2</sub> (observed by IR), α-SiO<sub>2</sub>=α-cristobalite

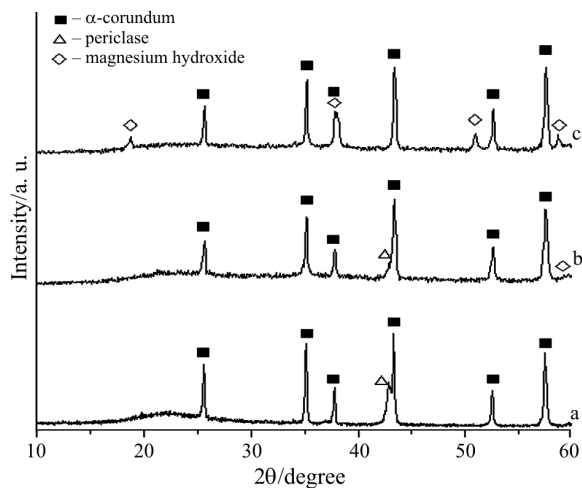


**Fig. 4** X-ray powder diffraction patterns of samples a – βaD4, b – βbD4, c – βcD4, d – βaD5, e – βbD5, f – βcD5 dried at 393 K

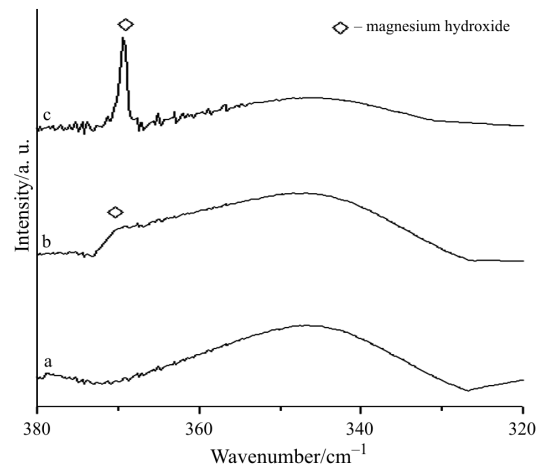


**Fig. 5** IR spectra of samples a – βaD4, b – βbD4, c – βcD4, d – βaD5, e – βbD5, f – βcD5 dried at 393 K

compared to αD5 sample (Fig. 1) these βD samples contain a higher amount of enstatite. The analysis of X-ray diffraction patterns and IR spectra also indicated that the amount of enstatite formed in the βaD5 sample

was larger than that formed in the βaD4 sample, and that the amount of forsterite was larger in βaD4 than in βaD5. In addition, the absence of XRD peaks at  $2\theta=22.90, 32.30, 35.70$  and  $39.80^\circ$  demonstrated that

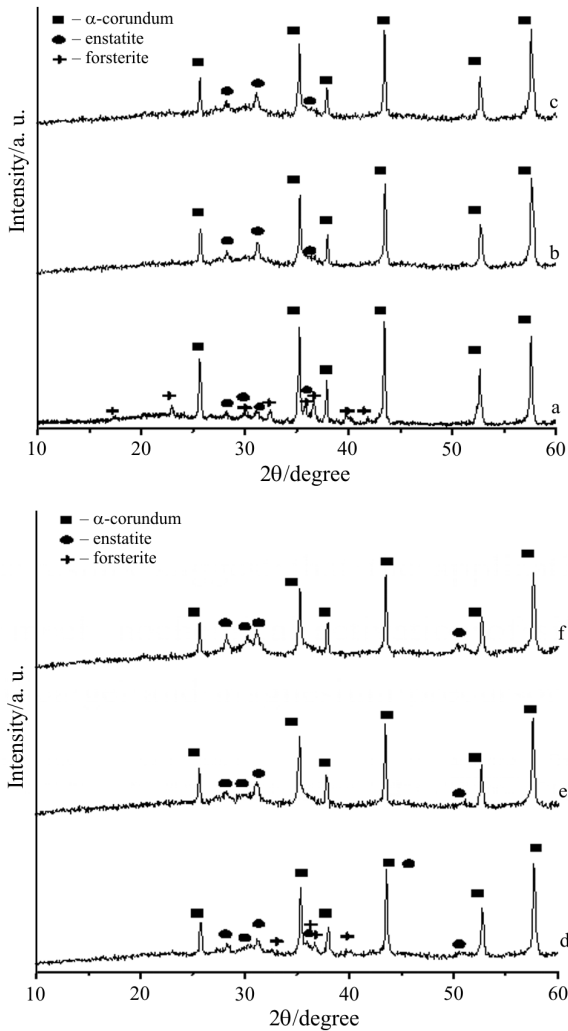


**Fig. 6** X-ray powder diffraction patterns of samples a –  $\beta$ aD4, b –  $\beta$ bD4, c –  $\beta$ cD4, d –  $\beta$ aD5, e –  $\beta$ bD5, f –  $\beta$ cD5 calcined at 1223 K

there was no forsterite formation [19] in those samples where the activation have been done in the presence of water ( $\beta$ bD4,  $\beta$ bD5,  $\beta$ cD4 and  $\beta$ cD5). Therefore, it can be affirmed that a decrease in the  $M/C$  ratio and an increase in the amount of water in the ‘activation medium’ result in an increase in the amount of enstatite formed, as well inhibited forsterite formation.

The above results suggest that the application of water as ‘activation medium’ allowed a higher degree of mechanochemical activation of silica gel and MgO, resulting an increase in the reaction between silica gel and magnesium precursor at 1223 K. The final result is the formation of enstatite and the inhibition of spinel formation, since the entire magnesium precursor probably reacted with silica gel.

As it can be seen in the Figs 7 and 8 (X-ray diffraction patterns and IR spectra), when these samples are calcined at 1523 K some XRD peaks appear at

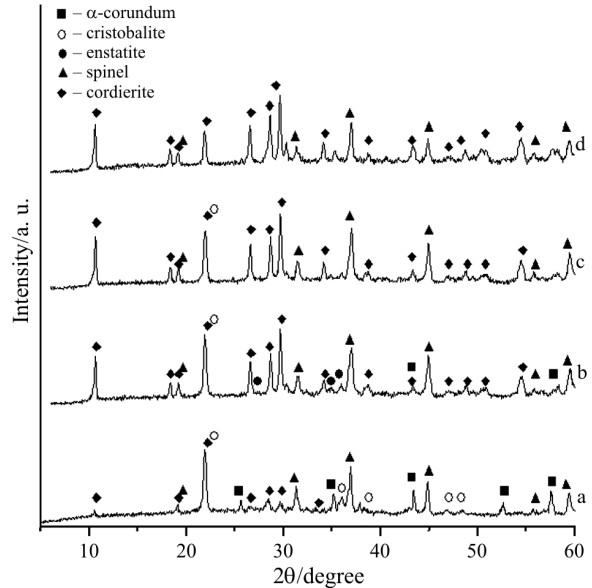


**Fig. 7** X-ray powder diffraction patterns of samples a –  $\beta$ aD0, b –  $\beta$ aD5, c –  $\beta$ bD5, d –  $\beta$ cD5 calcined at 1523 K

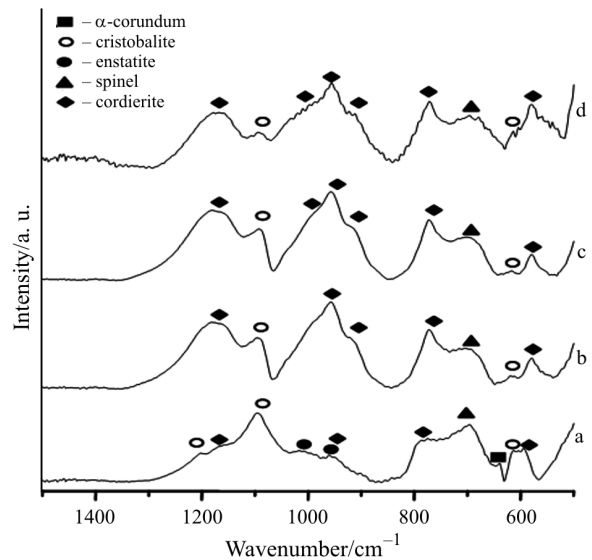


**Fig. 8** IR spectra of samples a –  $\beta$ aD0, b –  $\beta$ aD5, c –  $\beta$ bD5, d –  $\beta$ cD5 calcined at 1523 K

$2\theta=10.50$  and  $28.49^\circ$  and IR bands are observed at  $1179$ ,  $960$  and  $770\text{ cm}^{-1}$ , confirming the formation of the cordierite [17, 25–27]. In addition, an increase in the intensity of these peaks and bands, a gradual decrease in the intensity of cristobalite IR band at  $1090\text{ cm}^{-1}$  [22, 23] is observed which indicates that the silica consumption is associated with the formation of cordierite. When the degree of mechanochemical activation and the amount of water in the ‘activation medium’ increased the XRD peaks related to enstatite and  $\alpha$ -Al<sub>2</sub>O<sub>3</sub> have been gradually disap-

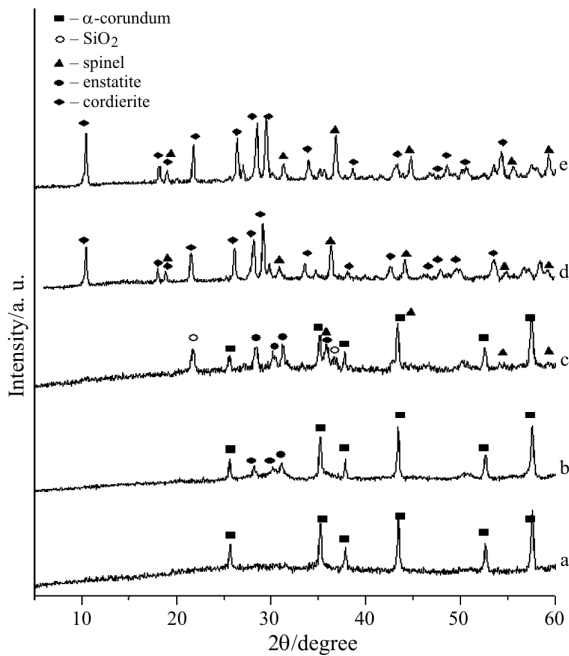


**Fig. 9** X-ray powder diffraction patterns of sample  $\beta cD5$  grounded and dried at a – 393, b – 1223, c – 1423, d – 1523 and e – 1623 K

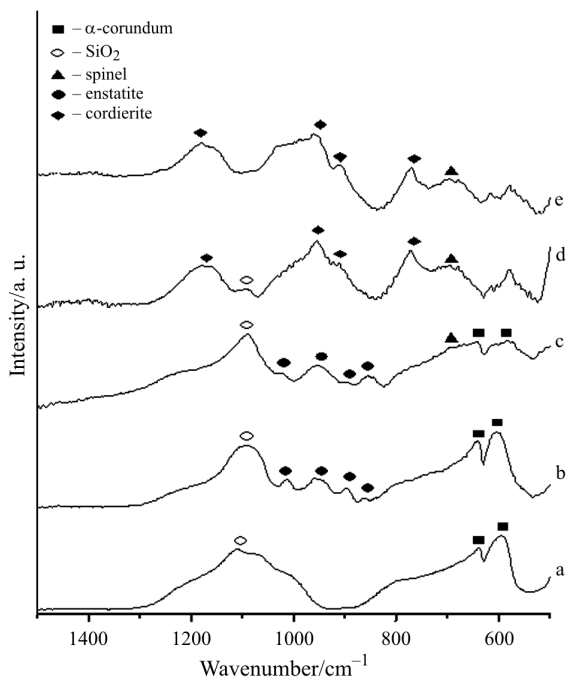


**Fig. 10** IR spectra of sample  $\beta cD5$  grounded and dried at a – 393, b – 1223, c – 1423, d – 1523 and e – 1623 K

peared. Therefore, the formation of cordierite is also associated with the consumption of these phases. Formation of  $MgAl_2O_4$  phase in all samples, proved by the XRD peaks at  $2\theta=36.80, 44.80, 59.40^\circ$  [15] and an IR band at  $690\text{ cm}^{-1}$  [21], was also observed. This phase was in a higher amount in  $\beta dD5$  sample.

X-ray diffraction patterns and IR spectra are presented in Figs 9 and 10 and illustrate the formation of different phases in  $\beta cD5$  sample as a function of temperature. For the sample, ground and dried at 393 K, the X-ray diffraction pattern (Fig. 9a) indicates that  $\alpha\text{-Al}_2\text{O}_3$  [14] is the only crystalline phase. The IR spectrum (Fig. 10a) indicates the presence of  $\alpha\text{-Al}_2\text{O}_3$  at  $640$  and  $590\text{ cm}^{-1}$ , and of amorphous  $\text{SiO}_2$  represented by a characteristic band around  $1110\text{ cm}^{-1}$ . The amorphous magnesium hydroxide –  $Mg(OH)_2$ , is indicated by the presence of IR band around  $3700\text{ cm}^{-1}$  (Fig. 5f). There are also several shoulders can be associated to other amorphous phases, e.g. to the amorphous magnesium silicate observed by MacKenzie for the  $MgO\text{-SiO}_2$  system [29]. When the sample was treated at 1223 K, an expressive amount of enstatite is formed (Fig. 9b). Besides the bands representing the  $\alpha\text{-Al}_2\text{O}_3$  (Fig. 10b) another IR band around  $1110\text{ cm}^{-1}$  evidencing the presence of amorphous  $\text{SiO}_2$ . For the sample calcined at 1423 K, the XRD peaks and IR bands indicated the  $\alpha\text{-cristobalite}$  [22–24],  $\alpha\text{-Al}_2\text{O}_3$  [14, 16], enstatite [19, 20] and a small amount of  $MgAl_2O_4$  [15, 21]. For the sample treated at 1523 K, the IR band at  $1090\text{ cm}^{-1}$  [22, 23] almost disappeared, which indicates a pronounced consumption of  $\text{SiO}_2$  (Fig. 10d). The main peaks observed in the X-ray diffraction pattern of this sample, are referring to cordierite [27], as major phase, and to the  $MgAl_2O_4$  [21], as minor phase. For the sample calcined at 1623 K, there are no significant alterations in the X-ray diffraction patterns and in the IR spectrum with regard to the sample heated at 1523 K. Therefore, the composition of this sample is basically cordierite and  $MgAl_2O_4$  as major and minor phases, respectively.

From the obtained results it is evident that the formation of enstatite at 1223 K has the major influence on the temperature and reaction pathway of cordierite formation. It is also clear that the degree of mechanochemical activation and the amount of water in the ‘activation medium’ are the most important factors on the formation of enstatite. Similar results were reported when the synthesis of cordierite was done in the presence of additives such as fluorite [11] or when the mechanochemical activation was made in an attrition mill at 4500 rpm and clay minerals were used as starting materials [30]. However, none of the above cited papers mentioned clearly the importance of enstatite on the process of cordierite formation.

With regard to the influence of spinel phase on the cordierite formation, some authors proposed that cordierite should be formed from the reaction between spinel and a silica precursor at around 1600 K [9]. Our results show that for the samples with high degree of mechanochemical activation the spinel phase do not participate on the cordierite formation.

## Conclusions

From the results obtained by XRD and IR spectroscopy, it was concluded:

- Conditions of grinding with  $t=18$  h or  $M/C$  higher than 1/40 do not present good results on the cordierite (Mg<sub>2</sub>Al<sub>4</sub>Si<sub>5</sub>O<sub>18</sub>) formation.
- In the aspect of cordierite synthesis, silica gel as SiO<sub>2</sub> precursor was found functioning better than dehydrated and calcined silicic acid.
- During the mechanochemical activation, in the samples where water was used as ‘activation medium’ the formation of Mg(OH)<sub>2</sub> promotes also the formation of enstatite (MgSiO<sub>3</sub>).
- In samples with high degree of mechanochemical activation, the formation of cordierite at 1523 K can be described by the following reaction:  
 $2\text{MgSiO}_3 + 2\text{Al}_2\text{O}_3 + 3\text{SiO}_2 \rightarrow \text{Mg}_2\text{Al}_4\text{Si}_5\text{O}_{18}$ .
- The mechanochemical activation, using water as ‘activation medium’, allows a great amount of cordierite formed at 1523 K.

## References

- 1 J. Temuujin, K. Okada and K. J. D. MacKenzie, *J. Eur. Ceram. Soc.*, 18 (1998) 831.
- 2 A. Z. Juhász, *Colloids Surf. A: Physicochem. Eng. Aspects*, 141 (1998) 449.
- 3 J. Temuujin, K. J. D. MacKenzie, M. Schmücker, H. Schneider, J. McManus and S. Winperis, *J. Eur. Ceram. Soc.*, 20 (2000) 413.
- 4 M. Senna, *Mater. Sci. Eng. A*, 304–306 (2001) 39.
- 5 V. V. Boldyrev, *Powder Technol.*, 122 (2002) 247.
- 6 J. Alkebro, S. Bégin-Clin, A. Mocellinb and R. Warren, *J. Solid State Chem.*, 164 (2002) 88.
- 7 S. Tamborenea, A. D. Mazzoni and E. F. Aglietti, *Thermochim. Acta*, 411 (2004) 219.
- 8 D. U. Tulyaganov, M. E. Tukhtaev, J. J. Escalante, M. J. Ribeiro and J. A. Labrincha, *J. Eur. Ceram. Soc.*, 22 (2002) 1775.
- 9 M. K. Naskar and M. Chatterjee, *J. Eur. Ceram. Soc.*, 24 (2004) 3499.
- 10 Z. M. Shi, K. M. Liang and S. R. Gu, *Mater. Lett.*, 51 (2001) 68.
- 11 S. Taruta, T. Hayashi and K. Kitajima, *J. Eur. Ceram. Soc.*, 24 (2004) 3149.
- 12 L. Stoch, *J. Therm. Anal. Cal.*, 77 (2004) 7.
- 13 Powder Diffraction File, JCPDS, Index card 4-0829 (1972).
- 14 Powder Diffraction File, JCPDS, Index card 10-173 (1972).
- 15 Powder Diffraction File, JCPDS, Index card 5-0672 (1972).
- 16 M. T. Tsai, *Mater. Res. Bull.*, 37 (2002) 2213.
- 17 Fiveash Data Management, (1997).
- 18 Powder Diffraction File, JCPDS, Index cards 4-0768 and 4-0769 (1972).
- 19 B. D. Saksena, *Trans. Faraday Soc.*, 57 (1961) 242.
- 20 Powder Diffraction File, JCPDS, Index card 7-216 (1972).
- 21 N. W. Grimes, *Spectrochim. Acta*, 28A (1972) 2217.
- 22 M. Haccuria, *Bull. Soc. Chim. Belge*, 62 (1953) 428.
- 23 F. Matossi, *J. Chem. Phys.*, 17 (1949) 679.
- 24 Powder Diffraction File, JCPDS, Index card 4-0379 (1972).
- 25 B. Güttler, E. Salje and A. Putnis, *Phys. Chem. Miner.*, 16 (1989) 365.
- 26 Gouby, P. Thomas, D. Mercurio, T. Merle-Méjean and B. Frit, *Mater. Res. Bull.*, 30 (1995) 593.
- 27 Powder Diffraction File, JCPDS, Index card 12-303 (1972).
- 28 Powder Diffraction File, JCPDS, Index card 7-239 (1972).
- 29 J. Temuujin, K. Okada and K. J. D. MacKenzie, *J. Solid State Chem.*, 138 (1998) 169.
- 30 F. A. Costa Oliveira and J. Cruz Fernandes, *Ceram. Int.*, 28 (2002) 79.

---

Received: July 5, 2005

Accepted: November 25, 2005

---

DOI: 10.1007/s10973-005-7405-1